Measured Channel Capacity of SIMO-UWB for Intra-Vehicle Communications

Fengzhong Qu[1], Jia Li[2], Liuqing Yang[3], and Timothy Talty[4]
[1]Department of Ocean Science and Engineering, Zhejiang University, Hangzhou, China,
Email: jimqufz@gmail.com
[2]Department of Electrical and Computer Engineering, Oakland University, Rochester, MI 48309,
Email: li4@oakland.edu, Tel: +1 248 370 2661, Fax: +1 248 370 4633
[3]Department of Electrical and Computer Engineering, Colorado State University,
1373 Campus Delivery, Fort Collins, CO 80523-1373,
Email: lqyang@engr.colostate.edu, Tel: +1 970 491 6215, Fax: +1 970 491 2249
[4]ECI Laboratory, General Motors Research and Development Center, Warren, MI 48090, Email: t.j.talty@ieee.org

Abstract— **The rapid progresses made in the area of intelligent transportation systems (ITS) call for high rate intra-vehicle wireless communications. Ultra wideband (UWB) and multi-antenna are both promising technologies providing high data rate. This paper evaluates the channel capacity of intra-vehicle single-input multiple-output (SIMO)-UWB using the measured signals in the experiment. The channel measurement is carried out in two vehicles, a sedan Ford Taurus and an SUV GM Escalade, with different transceiver placements, beneath the chassis and inside the engine compartment. Both channel state information available to the transmitter (CSIT) and channel state information available to the receiver (CSIR) cases are involved in our results. The results reveal that the channel capacity remain unchanged although experiment settings changes, including vehicle type, engine status, and transceiver location; and that water filling fails to demonstrate its advantage as the number of receiver antenna increases.**

I. Introduction

In recent years, intelligent transportation systems (ITS) attract more and more interests by improving the current transportation systems in all aspects. Intelligent transportation spaces (ITSp) integrate multiple ITS modules, as well as the participants and devices in transportation into spaces with distributed and pervasive intelligence [1]. Those participants and devices include various intra-vehicle ones, such as sensors for the vehicles and passengers, driving assistance devices, multimedia devices, etc. Since the pervasive intelligence in ITSp requires computational data exchange, high rate intra-vehicle wireless communications become a key enabler for ITSp.

In 2002, FCC authorized the unlicensed use of ultra-wideband (UWB) on the band from 3.1GHz to 10.6GHz with the emission limit as low as -41.3dBm/Hz that is the same limit applies to unintentional emitters. This huge bandwidth supports high data rate communications up to 480 Mbps over a short distance of $10-15$m at very low power levels. The extremely wide transmission bandwidth of UWB provides fine time resolution, which is an enabler of multipath diversity collection. The wide bandwith with low transmission power also provides resistance to narrowband interference. Furthermore, UWB radio have several unique advantages, including enhanced capability to penetrate obstacles, localization precision down to the centimeter level, very high data rates and high user capacity, small low latency, and potentially small device size and processing power [2].

The advantages of UWB open a door for high data rate intra-vehicle wireless communications and intra-vehicle UWB becomes a hot area. Since 2006, research on intra-vehicle UWB channel measurement, experiment, statistics, and other related results have been published consecutively. Ref. [3] compared the measured intra-vehicle channel in experiments with the channel model described in IEEE 802.15.3a. Ref. [3] plotted the root mean squared (RMS) delay distributions of the measured intra-vehicle channels and those of models given by IEEE 802.15.3a, and concluded that indoor models are not suitable for the UWB channels within commercial vehicles. Some channel statistics, such as maximum excess delay, RMS delay and the number of multipath components are theoretically derived [4]. The results in [5] show that the received signals within the vehicle are stable and high data rate UWB system can be implemented intra-vehicle. In [6], we reported our work in measuring and modeling the UWB propagation channel in commercial vehicles with different transceiver locations, beneath the chassis and inside the engine compartment. It is observed that paths arrive in clusters in the latter environment but such clustering phenomenon does not exist in the former case.

In indoor environments, multi-input multi-output (MIMO) schemes have long been used to provide improved capacity and accordingly enhanced data rates, such as IEEE 802.11n. In recent years, motivated by the increasing requirements of data rate and reliability of wireless transmissions, MIMO-UWB appeals growing interests [7]. Ref. [7] gives an overview of MIMO-UWB systems. The channel models and measured channel capacity are reported in [8]–[11]. However, most of them are for indoor environments except [8] in a rectangular metal cavity. As a result, very limited MIMO-UWB research has been done for intra-vehicle environments, which are very different from the indoor ones. The intra-vehicle channel faces particularly harsh multipath and shadowing constraints. The closed or semi-closed metallic intra-vehicle structure makes the compartments reverberation chambers, but with some regions shielded from other regions [12]. Moreover, the placement of antennas is highly constrained for the limited intra-vehicle space. All these pose challenges for high rate intra-vehicle MIMO communications. Ref. [12] evaluates MIMO performance for intra-vehicle communications in aircraft and cars with a focus on low data rates.

This paper presents our subsequent work of [6]. In this paper, measured results in the experiments in [6] are used to evaluate the channel capacity of intra-vehicle single-input multiple-output (SIMO)-UWB systems. The SIMO results in this paper can be regarded as preliminary work of MIMO systems. Our results cover channel state information available to the transmitter (CSIT) and channel state information available to the receiver (CSIR) cases. In the CSIT case, water filling is done at the transmitter for energy allocation on the frequency band while in the CSIR case, the transmit energy can only be allocated evenly on the entire band. The results reveal that although different settings, such as vehicle type, engine status, and transceiver locations, play important roles in channel characteristics, they hardly affect the channel capacity. In addition, water filling does not show its advantage as the number of receiver antenna increases. In most cases in our experiments, CSIT and CSIR have very close channel capacity when the number of receiver antennas is 3 or more.

The content of this paper is organized as follows: the next section introduces the system model. Section III presents the intra-vehicle UWB experiment settings. Section IV presents measured SIMO channel capacity. Finally, Section V gives concluding remarks.

II. System Model

A. Channel Model

In [6], we used different UWB channel models for the cases when the transceivers are beneath the chassis and inside the engine compartment because the channel statistics vary. Since this paper focuses on the channel capacity, for simplicity, the SIMO UWB channels with N receive antennas are modeled as an extension of the single-input single-output (SISO) case in [7]

$$h_n(t) = \sum_{l=1}^{L} \alpha_{nl} \delta(t - \tau_{nl}), \tag{1}$$

where $h_n(t)$ is the impulse response of the physical channel, δ the Dirac delta function, $n = 1, 2 \ldots N$ the index of the receive antennas, l, L, and τ_{nl} the index, number, and the according delay of multipath, and α_{nl} the amplitude. Since the real impulse is transmitted in UWB systems, α_{nl} is a real number.

B. Channel Capacity

Let

$$H_n(f) = \sum_{l=1}^{L} \alpha_{nl} e^{-j2\pi f (l-1)\tau_{nl}} \tag{2}$$

be the spectrum of $h_n(t)$ and the vector form $\boldsymbol{H} := [H_1(f), \ldots, H_N(f)]$. Let $S(f)$ be the power spectrum density (PSD) function of the transmitted signal $X(t)$ with the power constraint

$$\int_B S(f) df = S, \tag{3}$$

where B is the signal pass band.

Since UWB systems are wideband, the capacity is obtained by the integration in the frequency domain. The capacity with given $\boldsymbol{H}(f)$ is

$$C = \max_{\int_B S(f)df = S} \int_B \log_2 \left(1 + \frac{S(f)\boldsymbol{H}(f)\boldsymbol{H}^H(f)}{N_0} \right) df, \tag{4}$$

where N_0 is the noise PSD and $(\cdot)^H$ denotes the matrix Hermitian.

In the CSIT case, the channel information is available at the transmitter so that the optimum $S(f)$ is achieved by water filling as [11]

$$S(f) = \left[\Theta - \frac{N_0}{\boldsymbol{H}(f)\boldsymbol{H}^H(f)} \right]_+, \tag{5}$$

where $[\cdot]_+$ means only taking the value that is greater than or equal to 0 and Θ is a constant that satisfies

$$\int_{f \in F_\Theta \cap B} \left(\Theta - \frac{N_0}{\boldsymbol{H}(f)\boldsymbol{H}^H(f)} \right) df = S \tag{6}$$

with F_Θ the range of f in which $S(f) > 0$.

In the CSIR case where the channel information is only available at the receiver, the only thing the transmitter can do is to equally distribute the power throughout the band. Hence, the capacity of CSIR is accordingly

$$C = \int_B \log_2 \left(1 + \rho \boldsymbol{H}(f)\boldsymbol{H}^H(f) \right) df, \tag{7}$$

where ρ is the signal-to-noise ratio (SNR).

III. Experiment Settings

The measurement is performed in time domain by sounding the channel with narrow pulses and recording their responses with a digital oscilloscope. The block diagram in Fig. 1 illustrates the connections of the measurement apparatus. At the transmitter, a Wavetek sweeper along with an impulse generator from picosecond works to produce narrow pulses of width 100 picoseconds, as shown in Fig. 2. These pulses are fed into a scissors-type antenna, as shown in Fig. 3. At the receiving side, a digital oscilloscope of 15GHz bandwidth from Tektronix is connected to the receive antenna to record the received signals. The channel measurement was carried out in two vehicles, a sedan Ford Taurus and an SUV GM Escalade, with different transceiver placements, beneath the chassis and in the engine compartment.

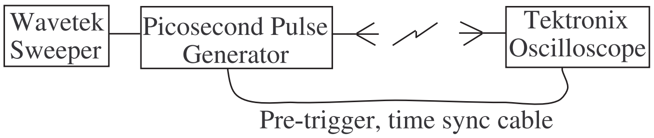

Fig. 1. Connections of channel sounding apparatus

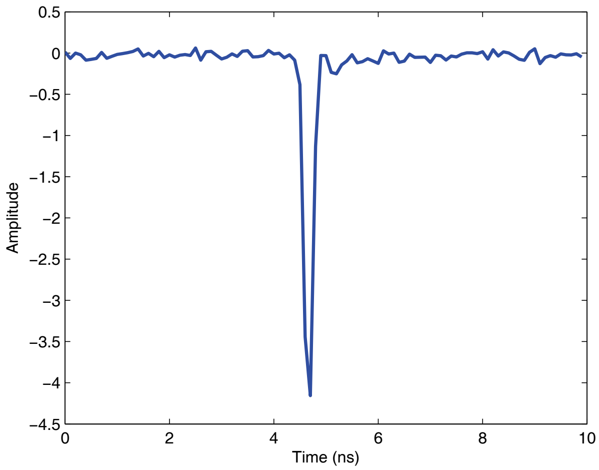

Fig. 2. The sounding pulse in the experiment

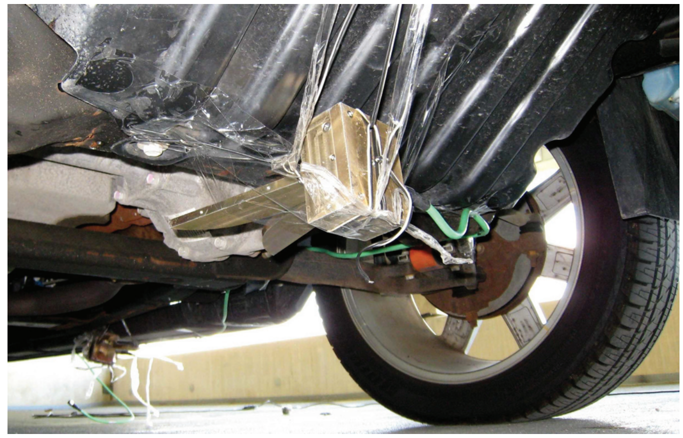

Fig. 3. The antenna in the experiment

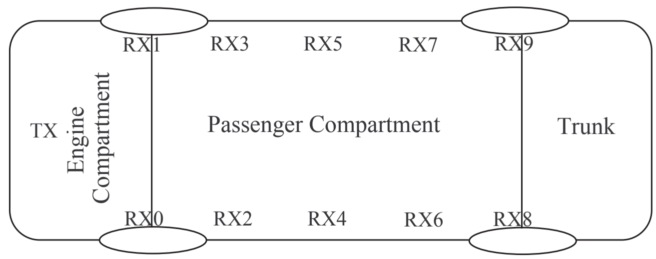

Fig. 4. Antenna locations for the measurements beneath the chassis

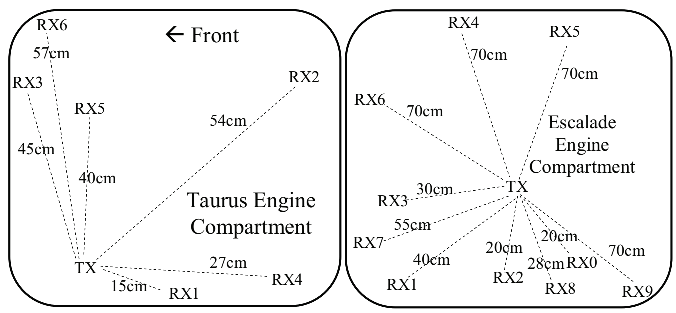

Fig. 5. Antenna locations for the measurements inside the engine compartment

In the first phase of the experiment, both the transmit and receive antennas were beneath the chassis and 15cm above the ground. The antennas are set to face each other and the line-of-sight (LOS) path always exists. Fig. 4 illustrates the locations of antennas. The transmit antenna was fixed at Location TX in the front, beneath the engine compartment. The receive antenna was moved to ten different spots, from RX0 to RX9. Five of them are located in a row along the left side of the vehicle, with equidistance of 70cm for the Taurus and 80cm for the Escalade between the neighboring spots. The other five sit symmetrically along the right side. The distance between TX and RX1 is 45cm for the Taurus and 50cm for the Escalade. For each receiver position, ten waveforms were recorded when pulses were transmitted repeatedly. Fig. 6 illustrates a recorded waveform beneath the Escalade chassis.

In the second phase, both the transmit and receive antennas were inside the engine compartment with closed hood. The positions of antennas highly depend on the available space in the compartment. Due to the difference between the engine compartment structures of Taurus and Escalade, the arrangements of antenna positions are different as shown in Fig. 5. For both vehicles, the transmit antenna had a fixed location and the receive antenna was moved to different spots. The engine compartments are full of metal auto components and there are always iron parts sitting between the antennas. Ten waveforms were recorded for each position of the receive antenna. Fig. 7 illustrates a recorded waveform inside the Escalade engine compartment.

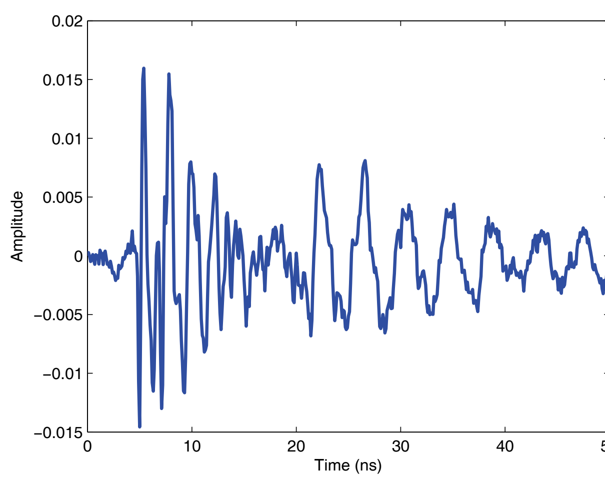

Fig. 6. A waveform recorded at location RX0 beneath the Escalade chassis

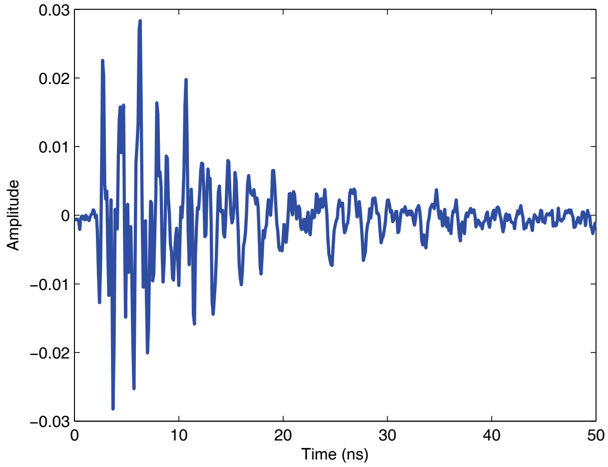

Fig. 7. A waveform recorded at location RX0 inside the Escalade engine compartment

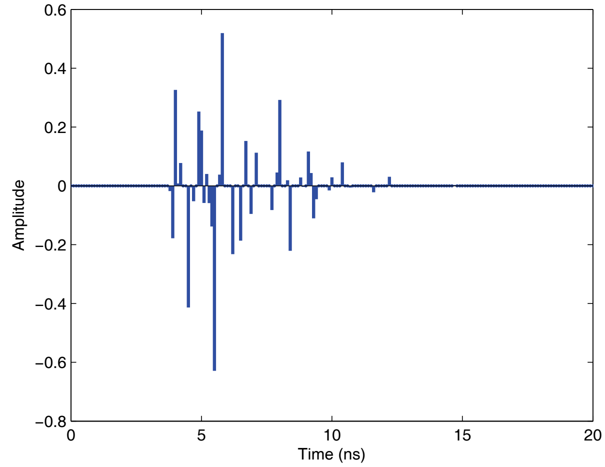

Fig. 9. Channel impulse response at location RX0 inside the Escalade engine compartment

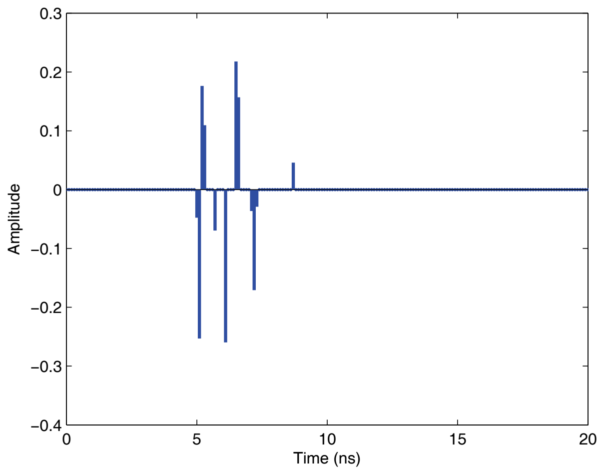

Fig. 8. Channel impulse response at location RX0 beneath the Escalade chassis

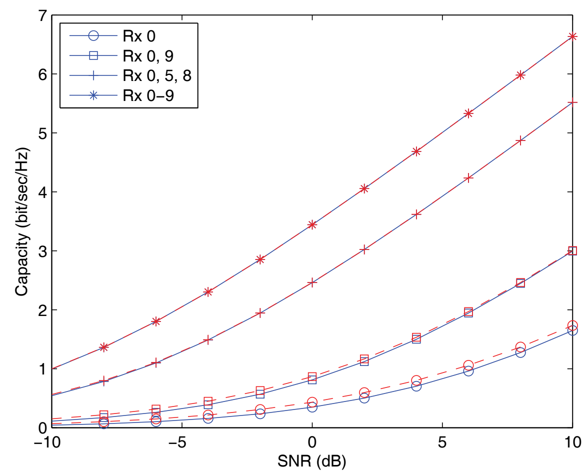

Fig. 10. Capacity of the channels beneath the Escalade chassis with the engine on. Solid: CSIR; Dashed: CSIT.

IV. Experiment Results

The channel impulse response is extracted from the recorded signals using the CLEAN algorithm as in [6]. The deconvolved channel impulse response according to Figs. 6 and 7 are shown in Figs. 8 and 9. The figures show that the channel inside the engine compartment suffers from more severe multipath.

The channel capacity with 1, 2, 3, and all 10 (6 for the channels inside the Taurus' engine compartment) receive antennas in different settings are plotted Figs. 10 – 14. It is observed that in these figures, when there is only 1 receiver antenna, the channel capacity with CSIT is remarkably larger than that with CSIR. As the the number of the receive antennas increases, this advantage vanishes in every scenario and becomes hard to tell since the number of the receiver antennas reaches 3.

Another observation is that with a single or a few receive antennas, there are notable channel capacity differences among different scenarios because of different channel statistics. As the number of the receive antennas increases, these differences diminish. In the cases using all 10 receiver antennas, the capacity of different scenarios becomes identical.

These two observations provide essential reference in intra-vehicle SIMO-UWB system designs. As the number of the receive antennas reaches a certain number, say 3 or more, both the channel state information at the transmitter and the channel statistics become unimportant in terms of channel capacity.

V. Conclusions

In this paper, the channel capacity of intra-vehicle SIMO-UWB is evaluated by employing the measured signals in the experiment. The experiment is conducted by sounding the channel with narrow pulses and recording their response with a digital oscilloscope. The channel measurement is carried out in two types of vehicles, an Escalade and a Taurus, with different transceiver locations, beneath the chassis and inside the engine compartment. Our results cover both CSIT and CSIR cases, revealing that as the number of the receive

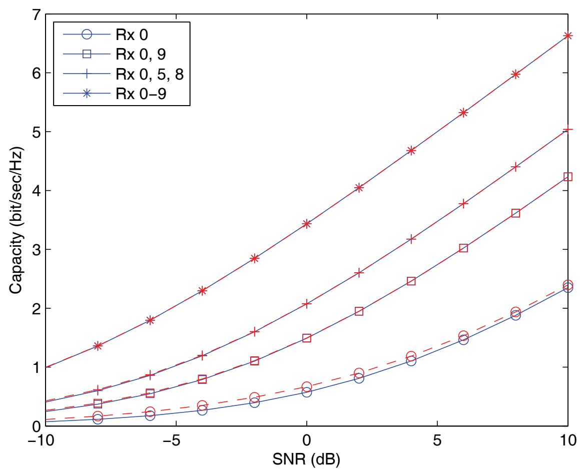

Fig. 11. Capacity of the channels beneath the Escalade chassis with the vehicle running on road. Solid: CSIR; Dashed: CSIT.

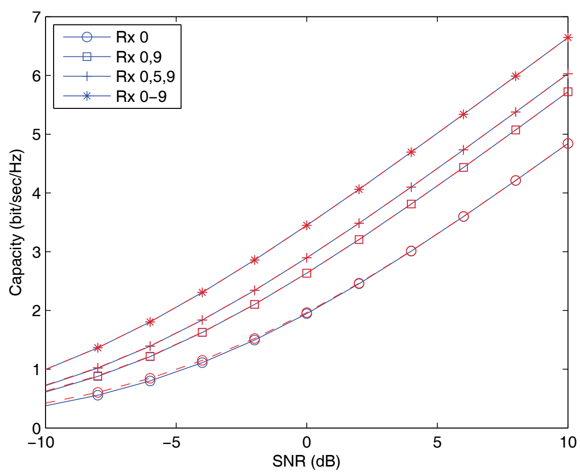

Fig. 12. Capacity of the channels beneath the Taurus chassis with the engine on. Solid: CSIR; Dashed: CSIT.

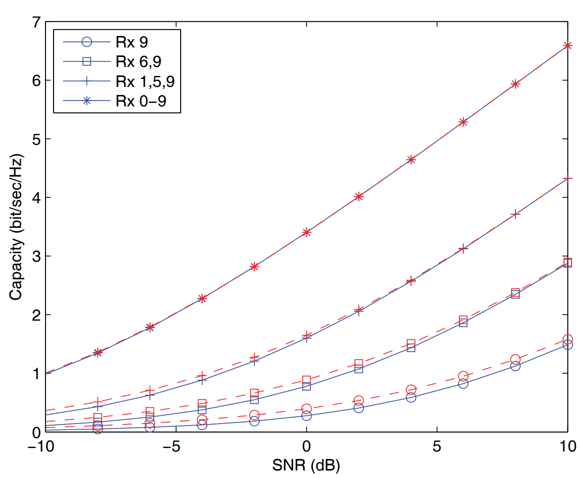

Fig. 13. Capacity of the channels inside the Escalade's engine compartment with the engine on. Solid: CSIR; Dashed: CSIT.

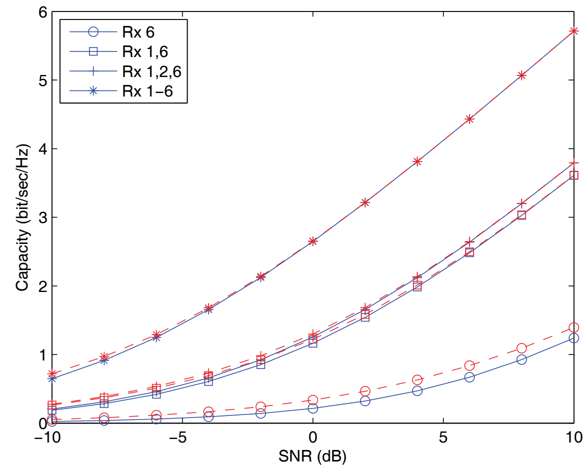

Fig. 14. Capacity of the channels inside the Taurus' engine compartment with the engine off. Solid: CSIR; Dashed: CSIT.

antennas reaches a certain number, say 3 or more, both the channel state information at the transmitter and the channel statistics become unimportant in terms of channel capacity.

REFERENCES

[1] F. Qu, F. Wang, and L. Yang, "Intelligent transportation spaces: vehicles, traffic, communications, and beyond," *IEEE Communications Magazine*, vol. 48, no. 11, pp. 136–142, November 2010.

[2] L. Yang and F. Wang, "Driving into intelligent spaces with pervasive communications," *IEEE Intelligent Systems*, vol. 22, no. 1, pp. 12–15, January-February, 2007.

[3] W. Aldeeb, W. Xiang, and P. Richardson, "A study on the channel and BER-SNR performance of ultra wide band systems applied in commercial vehicles," in *Proc. of IEEE Sarnoff Symposium*, Princeton, NJ, April 30-May 2, 2007.

[4] W. Xiang, "A vehicular ultra-wideband channel model for future wireless intra-vehicle communications (IVC) systems," in *Proc. of Vehicular Technology Conf.*, Baltimore, MD, September 30-October 3, 2007.

[5] J. Li and T. Talty, "Channel characterization for ultra-wideband intra-vehicle sensor networks," in *Proc. of IEEE Military Communications Conference*, Washington, DC, October 23-25, 2006.

[6] W. Niu, J. Li, and T. Talty, "Ultra-wideband channel modeling for intravehicle environment," *EURASIP Journal on Wireless Communications and Networking*, vol. 2009, doi:10.1155/2009/806209.

[7] T. Kaiser, F. Zheng, and E. Dimitrov, "An overview of ultra-wide-band systems with MIMO," *Proceedings of the IEEE*, vol. 97, no. 2, pp. 285–312, February 2009.

[8] Z. Hu, D. Singh, and R. Qiu, "MIMO capacity for UWB channel in rectangular metal cavity," in *Proc. of IEEE Southeastcon*, Huntsville, AL, April 3-6, 2008.

[9] W. Q. Malik and D. J. Edwards, "Measured MIMO capacity and diversity gain with spatial and polar arrays in ultrawideband channels," *IEEE Trans. on Communications*, vol. 55, no. 12, pp. 2361–2370, December 2007.

[10] M. Migliore, D. Pinchera, A. Massa, R. Azaro, F. Schettino, and L. Lizzi, "An investigation on UWB-MIMO communication systems based on an experimental channel characterization," *IEEE Transactions on Antennas and Propagation*, vol. 56, no. 9, pp. 3081–3083, September 2008.

[11] F. Zheng and T. Kaiser, "On the evaluation of channel capacity of UWB indoor wireless systems," *IEEE Transactions on Signal Processing*, vol. 56, no. 12, pp. 6106–6113, December 2008.

[12] A. Magleby and C. Furse, "Predicted MIMO performance in intra-vehicle channels," in *IEEE Antennas and Propagation Society International Symposium*, San Diego, CA, July 5-11, 2008.